Windowed All Phase Biorthogonal Transform and Its Application in JPEG-Like Image Compression

Qiming Fu, Xiao Zhou, Chengyou Wang, and Baochen Jiang
School of Mechanical, Electrical and Information Engineering, Shandong University, Weihai 264209, China
Email: fqmsdu@163.com; {zhouxiao, wangchengyou, jbc}@sdu.edu.cn

Abstract —This paper proposes new concepts of the windowed all phase biorthogonal transform (WAPBT), which is inspired by the all phase biorthogonal transform (APBT). In the light of windowed all phase digital filter theory, windowed all phase biorthogonal transforms is proposed. The matrices of WAPBT based on DFT, WHT, DCT and IDCT are deduced, which can be used in image compression instead of the conventional DCT, and the image compression scheme proposed in this paper is called WAPBT-based JPEG (WAPBT-JPEG). With optimal window sequence of WAPBT for image compression obtained by using generalized pattern search algorithm (GPSA), the peak signal to noise ratio (PSNR) and visual quality of the reconstructed images using the WAPBT-JPEG is outgoing DCT-based JPEG (DCT-JPEG) and APBT-based JPEG (APBT-JPEG) approximately at all bit rates. What is more, by comparison with DCT-JPEG, the advantage of proposed scheme is that the quantization table is simplified and the transform coefficients can be quantized uniformly. Therefore, the computing time becomes shorter and the hardware implementation is easier.

Index Terms—Windowed all phase biorthogonal transform (WAPBT), image compression, discrete cosine transform (DCT), JPEG algorithm, generalized pattern search algorithm (GPSA), windowed all phase digital filter (APDF)

I. Introduction

To achieve a greater convenience for image storage and transmission, the development of multimedia and internet requires a more suitable method for image compression. Discrete cosine transform (DCT) [1] has been adopted widely in international standards for image compression, for example, JPEG [2], MPEG-2 [3], MPEG-4 [4] and H.264/AVC [5]. In spite of the emerging wavelet-based standard JPEG2000 [6], the DCT-based JPEG standard remains to be the most commonly employed lossy compression algorithm for still images due to its high effectiveness and low computational complexity.

However, mathematical transforms and image compression are old but often changing topics [7], [8] in which a number of researchers have shown great interest over the last decade. In order to improve performance of image compression further, recently many new transforms used in image compression were proposed. In 2007 and in 2014, "peak transform" [9] and "discrete anamorphic transform" [10] were proposed successively based on different theory. Both of them are pre-transform (or pre-compression) techniques used before JPEG, JPEG2000, etc. Experimental results show that these pre-transform techniques used in image compression field can improve the performance of reconstructed images really significantly both in terms of PSNR and visual quality. However, with additional pre-transform algorithm, more complex calculation and processing time consumption are required. In 2008, "morphological transform" [11] was proposed, and it was used in image compression instead of the DCT. "Morphological transform" has a lower complexity in calculation comparing with DCT. However, a blemish in an otherwise perfect transform, experimental results have shown that the performance of reconstructed images is worse when "morphological transform" is used instead of the DCT. On the other hand, a kind of DCT-like transforms instead of DCT for image compression were studied in recent years [12]-[14]. This type of DCT-like transforms can be realized by few simple mathematical operations, but performance on reconstructed images is worse. In 2009, "all phase biorthogonal transform" (APBT) that was based on all phase digital filter theory was proposed by Hou *et al.* [15]. When APBT replaces DCT for the compression and reconstruction of image (called APBT-JPEG in [15]), similar performance was obtained, and it must be said that APBT-JPEG has good performance at low bit rates. Moreover, simple quantization is used in APBT-JPEG.

Inspired by the APBT, in this paper, we bring forward a new transform, namely the windowed all phase biorthogonal transform (WAPBT) that is based on windowed all phase digital filter theory [16]-[18]. The WAPBT is considered to be a more general transform for APBT. With optimal window sequence of WAPBT for image compression obtained by using generalized pattern search algorithm (GPSA) [19]-[22], it can be applied to image compression successfully instead of the conventional DCT. It can achieve better performance than APBT-JPEG, outgoing DCT-JPEG at various bit rates. Besides, by inheriting good properties from APBT-JPEG, the advantage of proposed scheme is that the quantization table is simpler; and the transform coefficients can be quantized uniformly, the computation

Manuscript received January 20, 2015; revised April 10, 2015.
This work was supported in part by the National Natural Science Foundation of China under Grant No. 61201371 and the promotive research fund for excellent young and middle-aged scientists of Shandong Province, China under Grant No. BS2013DX022.
Corresponding author email: zhouxiao@sdu.edu.cn.
doi:10.12720/jcm.10.4.284-293

simplified, and the computation time shortened. It can be easily implemented by software and hardware.

The rest of this paper is organized as follows. Section II introduces and concludes the principle of windowed all phase digital filter (APDF). Based on windowed APDF theory, windowed all phase biorthogonal transform (WAPBT) is proposed in Section III. And then in Section IV, the conventional DCT and JPEG image compression algorithm is introduced. The method to obtain optimal window sequence of WAPBT and the applications of WAPBT in image compression are described in Section V. In Section VI, experimental results and comparisons with conventional JPEG compression algorithm are presented; rate distortion curves of typical images are plotted; and some reconstructed images are also displayed. Finally, conclusions and discussions for further research are given in Section VII.

II. The Principle of Windowed All Phase Digital Filter

A. All Phase Philosophy

In this paper, the $\boldsymbol{\alpha}$ is a kind of transform such as DFT, WHT, DCT, and IDCT, and the $\boldsymbol{\alpha}_N$ is the $N\times N$ transform matrix corresponding to the transform $\boldsymbol{\alpha}$.

All phase philosophy can be considered to an application of overlap philosophy. For a digital sequence $\{x(n)\}$, there are N N-dimensional vectors. Each vector contains $x(n)$ and has different intercept phases:

$$\begin{aligned}
&\boldsymbol{X}_0 = [x(n), x(n+1), \cdots, x(n+N-1)]^{\mathrm{T}} \\
&\boldsymbol{X}_1 = z^{-1}\boldsymbol{X}_0 = [x(n-1), x(n), \cdots, x(n+N-2)]^{\mathrm{T}} \\
&\qquad\vdots \\
&\boldsymbol{X}_{N-1} = z^{-(N-1)}\boldsymbol{X}_0 = [x(n-N+1), x(n-N+2), \cdots, x(n)]^{\mathrm{T}}
\end{aligned} \tag{1}$$

where z^{-j} ($j=0,1,\cdots,N-1$) stands for the delay operator. Obviously, $x(n)$ is the intersection of $\boldsymbol{X}_i (i=0,1,\cdots,N-1)$, that is $x(n)=\boldsymbol{X}_0 \bigcap \boldsymbol{X}_1 \bigcap \cdots \bigcap \boldsymbol{X}_{N-1}$. According to the conventional representation of data matrices, the all phase data matrix of $x(n)$ is defined as $\boldsymbol{X}_{-N+1,0}(n)=[\boldsymbol{X}_0, \boldsymbol{X}_1, \cdots, \boldsymbol{X}_{N-1}]$, and an all phase data space of $x(n)$ is spanned by all the column vectors $\boldsymbol{X}_i (i=0,1,\cdots,N-1)$.

B. The Principle of Windowed All Phase Digital Filter (APDF) Based on $\boldsymbol{\alpha}$

APDF is a new scheme for 1-dimensional FIR filter design proposed at [17] in 2003, and its theory and application was researched further in recent years [23-26]. APDF is proposed based on all phase philosophy.

Architecture of the windowed APDF based on $\boldsymbol{\alpha}$ implemented directly in frequency domain is shown in Fig. 1.

Windowing is a kind of modulation for the signals. In Fig. 1, we add a front window $\boldsymbol{B}^1(n)$ $(n=0,1,\cdots,N-1)$ after the input signal $\{x(n)\}$ and a rear window $\boldsymbol{B}^2(n)$ before the output signal $y(n)$ respectively.

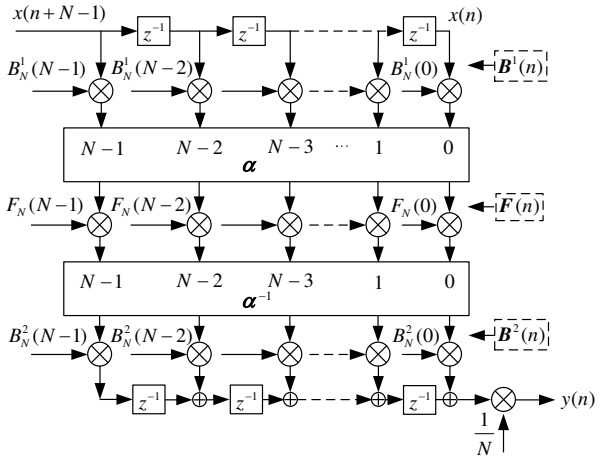

Fig. 1. Architecture of the windowed APDF based on $\boldsymbol{\alpha}$ implemented directly in $\boldsymbol{\alpha}$ domain.

$$\begin{aligned}
\boldsymbol{B}^1 &= [B_N^1(0), B_N^1(1), \cdots, B_N^1(N-1)]^{\mathrm{T}} \\
\boldsymbol{B}^2 &= [B_N^2(0), B_N^2(1), \cdots, B_N^2(N-1)]^{\mathrm{T}}
\end{aligned} \tag{2}$$

Particularly, when $\boldsymbol{B}^1(n)=\boldsymbol{1}$ and $\boldsymbol{B}^2(n)=\boldsymbol{1}$, the data without window can be regarded as the data with the rectangular window.

$\boldsymbol{F}$ is N-dimensional respected sequency response vector for windowed APDF based $\boldsymbol{\alpha}$,

$$\boldsymbol{F} = [F_N(0), F_N(1), \cdots, F_N(N-1)]^{\mathrm{T}} \tag{3}$$

$$\boldsymbol{S} = [\boldsymbol{s}_0, \boldsymbol{s}_1, \cdots, \boldsymbol{s}_{N-1}] \tag{4}$$

The matrix $\boldsymbol{S}$ with size of $N\times N$ is the extraction operator, where $\boldsymbol{s}_i (i=0,1,\cdots,N-1)$ is the i-th N-dimensional column vector. The i-th element in vector $\boldsymbol{s}_i$ is the value 1 and the rest elements are the value 0.

The relationship between input signal $x(n)$ and output signal $y(n)$ in windowed APDF based on $\boldsymbol{\alpha}$ is shown in Fig. 2.

$\boldsymbol{X}_i$ $(i=0,1,\cdots,N-1)$ is the i-th column vector of the all phase data matrix of $x(n)$. We can get a value $y^i(n)$ after $\boldsymbol{X}_i$ is filtered. That is:

$$y^i(n) = \boldsymbol{s}_i^{\mathrm{T}}\{\boldsymbol{B}^2 \cdot \{\boldsymbol{\alpha}^{-1}\{\boldsymbol{F} \cdot [\boldsymbol{\alpha}(\boldsymbol{B}^1 \cdot \boldsymbol{X}_i)]\}\}\} \tag{5}$$

where the mark "$\cdot$" represents dot product operation. According to Eq. (1) ~ Eq. (5), output signal can be expressed as:

$$\begin{aligned}
y(n) &= \frac{1}{N}\sum_{i=0}^{N-1} y^i(n) \\
&= \frac{1}{N}\sum_{i=0}^{N-1}\{\boldsymbol{s}_i^{\mathrm{T}}\{\boldsymbol{B}^2 \cdot \{\boldsymbol{\alpha}^{-1}\{\boldsymbol{F} \cdot [\boldsymbol{\alpha}(\boldsymbol{B}^1 \cdot \boldsymbol{X}_i)]\}\}\}\} \\
&= \sum_{i=0}^{N-1}\sum_{j=0}^{N-1}[B_N^2(i)A(i,j)B_N^1(j)x(n-i+j)]
\end{aligned} \tag{6}$$

where $A(i,j)=\frac{1}{N}\sum_{m=0}^{N-1}F_N(m)\alpha_N^{-1}(i,m)\alpha_N(m,j)$.

Eq. (6) can be written in the following form:

$$\begin{aligned} y(n) &= \sum_{i=0}^{N-1}\sum_{j=0}^{N-1}[B_N^2(i)A(i,j)B_N^1(j)x(n-i+j)] \\ &= \sum_{\tau=-(N-1)}^{N-1}[\sum_{i=\tau}^{\tau+N-1}H(i,i-\tau)]x(n-\tau) \\ &= \sum_{\tau=-(N-1)}^{N-1}h(\tau)x(n-\tau) \\ &= h(n)*x(n), \end{aligned} \tag{7}$$

where $H(i,j)=B_N^2(i)A(i,j)B_N^1(j)$. In the end, there is:

$$h(\tau)=\begin{cases}\sum_{i=\tau}^{N-1}H(i,i-\tau), & \tau=0,1,\cdots,N-1, \\ \sum_{i=0}^{\tau+N-1}H(i,i-\tau), & \tau=-1,-2,\cdots,-N+1,\end{cases} \tag{8}$$

From Eq. (8), what we can conclude above is that the unit impulse response of N-order windowed APDF based on $\boldsymbol{\alpha}$ is $\{h(\tau)\}$ $(\tau=-N+1,\cdots,0,\cdots,N-1)$. The N-order windowed APDF based on $\boldsymbol{\alpha}$ is equivalent to a FIR digital filter with the length of $2N-1$.

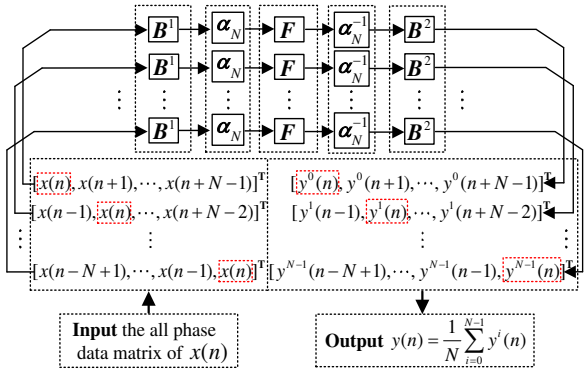

Fig. 2. The relationship between input signal $x(n)$ and output signal $y(n)$ in windowed APDF based on $\boldsymbol{\alpha}$.

C. The Condition of Zero-Phase FIR Filter

Under the condition of $H(i,j)=H(j,i)$, we will get $h(\tau)=h(-\tau),\ \tau=0,1,\cdots,N-1,$ which means that the APDF based on $\boldsymbol{\alpha}$ is a zero-phase FIR filter. When $\boldsymbol{\alpha}$ is orthogonal transform and $\boldsymbol{\alpha}_N$ is a real matrix ($\boldsymbol{\alpha}_N^{-1}=\boldsymbol{\alpha}_N^{\mathrm{T}}$), such as DCT, IDCT, WHT, the necessary and sufficient condition of $H(i,j)=H(j,i)$ is that $\boldsymbol{B}^2(n)=m\boldsymbol{B}^1(n)$, which can be proofed easily. m is a constant that can be value 1, which will not have an influence on $\{h(\tau)\}$.

When $\boldsymbol{\alpha}$ is DFT ($\boldsymbol{\alpha}_N$ is a complex matrix), $\boldsymbol{B}^1(n)=\boldsymbol{1}$ and $\boldsymbol{B}^2(n)=\boldsymbol{1}$, there is a fast algorithm to design APDF based on DFT, which is a zero-phase FIR filter [17]. The APDF based on $\boldsymbol{\alpha}$ (especially $\boldsymbol{\alpha}$ is DFT) is a new scheme for 1-dimensional FIR filter design, possessing concurrently the merits of the windowing and the frequency sampling methods. It is superior to the conventional methods in overall filter characteristics.

III. Windowed All Phase Biorthogonal Transform

A. The Derivation of Windowed All Phase Biorthogonal Transform (WAPBT)

$h(\tau)$ is an element of $\{h(\tau)\}$ that is the unit impulse response of N-order windowed APDF based on $\boldsymbol{\alpha}$. Define the vector $\boldsymbol{h}=[h(0),h(1),\cdots,h(N-1)]$, and $\boldsymbol{F}$ is N-dimensional respected sequency response vector for windowed APDF based $\boldsymbol{\alpha}$. From the principle of all phase digital filter (APDF) based on $\boldsymbol{\alpha}$, and according to Eq. (8), we have:

$$\begin{aligned} h(\tau) &= \sum_{i=\tau}^{N-1}H(i,i-\tau) \\ &= \sum_{i=\tau}^{N-1}B_N^2(i)A(i,i-\tau)B_N^1(i-\tau) \\ &= \sum_{i=\tau}^{N-1}B_N^2(i)B_N^1(i-\tau)[\frac{1}{N}\sum_{m=0}^{N-1}F_N(m)\alpha_N^{-1}(i,m)\alpha_N(m,i-\tau)] \\ &= \frac{1}{N}\sum_{i=\tau}^{N-1}\sum_{m=0}^{N-1}[B_N^2(i)B_N^1(i-\tau)F_N(m)\alpha_N^{-1}(i,m)\alpha_N(m,i-\tau)] \\ &= \sum_{m=0}^{N-1}[\frac{1}{N}\sum_{i=\tau}^{N-1}B_N^2(i)B_N^1(i-\tau)\alpha_N^{-1}(i,m)\alpha_N(m,i-\tau)]F_N(m) \\ &= \sum_{m=0}^{N-1}W(\tau,m)F_N(m),\quad \tau=0,1,\cdots,N-1. \end{aligned} \tag{9}$$

From Eq. (9), we have $\boldsymbol{h}=\boldsymbol{WF}$. Therefore, the transform $\boldsymbol{W}$ connects $\boldsymbol{\alpha}$ domain and time domain, and we call it **windowed all phase biorthogonal transform** (**WAPBT**). The elements in the transform matrix $\boldsymbol{W}$ are:

$$W(\tau,m)=\frac{1}{N}\sum_{i=\tau}^{N-1}B_N^2(i)B_N^1(i-\tau)\alpha_N^{-1}(i,m)\alpha_N(m,i-\tau) \tag{10}$$

where $\tau=0,1,\cdots,N-1,\ m=0,1,\cdots,N-1$.

When $\boldsymbol{\alpha}$ is orthogonal transform ($\boldsymbol{\alpha}_N$ is a real matrix) and $\boldsymbol{B}^2(n)=m\boldsymbol{B}^1(n)=\boldsymbol{B}(n),\ m=1$, we have $h(\tau)=h(-\tau),\ \tau=0,1,\cdots,N-1.$ The transform $\boldsymbol{W}$ called WAPBT strictly connects $\boldsymbol{\alpha}$ domain and time domain. In this case, the elements of the $\boldsymbol{W}$ are:

$$W(\tau,m)=\frac{1}{N}\sum_{i=\tau}^{N-1}B_N(i)B_N(i-\tau)\alpha_N(m,i)\alpha_N(m,i-\tau) \tag{11}$$

where $\tau=0,1,\cdots,N-1,\ m=0,1,\cdots,N-1$.

For 1-D vector $\boldsymbol{x}$, we define the WAPBT as $\boldsymbol{y}=\boldsymbol{Wx}$ and the inverse WAPBT (IWAPBT) $\boldsymbol{x}=\boldsymbol{W}^{-1}\boldsymbol{y}$. We define the 2-D WAPBT as $\boldsymbol{Y}=\boldsymbol{WXW}^{\mathrm{T}}$ and the IWAPBT is $\boldsymbol{X}=(\boldsymbol{W}^{-1})\boldsymbol{Y}(\boldsymbol{W}^{-1})^{\mathrm{T}}$, where $\boldsymbol{X}$ denotes an image matrix, $\boldsymbol{Y}$ denotes the matrix of transform coefficients.

B. Relationship between the WAPBT and APBT

Similar to APBT, WAPBT is a more general transform whose performance can be improved when proper window sequences are chosen. Particularly, when the

rectangular window is added ($\boldsymbol{B}^1(n)=\mathbf{1}$ and $\boldsymbol{B}^2(n)=\mathbf{1}$), the WAPBT is just so-called APBT. APBT ($\boldsymbol{\alpha}$ is IDCT) is a high efficient transform method of signal representation and has been applied successfully in image coding [15, 27]. According to Eq. (10) or (11), the elements of APBT matrix $\boldsymbol{V}$ are ($\boldsymbol{\alpha}$ is IDCT):

$$V(m,n)=\begin{cases}\dfrac{1}{N}, & m=0,\ n=0,1,\cdots,N-1,\\ \dfrac{N-m+\sqrt{2}-1}{N^2}\cos\dfrac{m(2n+1)\pi}{2N}, & m=1,2,\cdots,N-1,\\ & n=0,1,\cdots,N-1.\end{cases} \tag{12}$$

From Fig. 1 and Eq. (10), we can conclude that window sequences of WAPBT are some parameters that will change the nature of WAPBT. A kind of method to choose proper window sequences of WAPBT to improve its performance on image compression will be discussed in following sections.

IV. The Conventional DCT and JPEG Image Compression Algorithm

A. The Conventional DCT

The conventional 2-D DCT is always implemented separately by two 1-D DCTs. Let us use $\boldsymbol{X}$ and $\boldsymbol{C}$ to denote an image block and the DCT matrix with size of $N\times N$, respectively. After the conventional 2-D DCT, the transform coefficient block $\boldsymbol{Y}$ can be expressed as $\boldsymbol{Y}=\boldsymbol{C}\boldsymbol{X}\boldsymbol{C}^{\mathrm{T}}$, where $\boldsymbol{C}^{\mathrm{T}}$ is the transpose matrix of $\boldsymbol{C}$,

$$C(i,j)=\begin{cases}\sqrt{\dfrac{1}{N}}, & i=0,\ j=0,1,\cdots,N-1,\\ \sqrt{\dfrac{2}{N}}\cos\dfrac{i(2j+1)\pi}{2N}, & i=1,2,\cdots,N-1,\\ & j=0,1,\cdots,N-1.\end{cases} \tag{13}$$

Since DCT is an orthogonal transform, i.e. $\boldsymbol{C}^{\mathrm{T}}=\boldsymbol{C}^{-1}$, we use $\boldsymbol{X}=(\boldsymbol{C}^{-1})\boldsymbol{Y}(\boldsymbol{C}^{-1})^{\mathrm{T}}=\boldsymbol{C}^{\mathrm{T}}\boldsymbol{Y}\boldsymbol{C}$ to reconstruct the image.

B. DCT-based JPEG Image Compression Algorithm

The encoder of DCT-JPEG is mainly composed of four parts: forward discrete cosine transform (FDCT), quantization, zigzag scan, and entropy encoder. In the encoding process, the input image is grouped into blocks of size 8×8. Prior to computing the FDCT, the input image data are level shifted to a signed two's complement representation. For 8-bit input precision, the level shift is achieved by subtracting 128. And then, each block is transformed by the FDCT into 64 DCT coefficients, the DC coefficient and the 63 AC coefficients. After quantization, the DC coefficient of each block is coded in a differential pulse code modulation (DPCM). The 63 quantized AC coefficients are converted into a 1-D zig-zag sequence, preparing for entropy encoding. The decoder also contains four major parts: entropy decoder, inverse zig-zag scan, dequantization, and IDCT, which performs essentially the inverse of its corresponding main procedure within the encoder.

V. Application of WAPBT in Image Compression

A. Modified JPEG Algorithm Based on WAPBT

The proposed scheme of WAPBT-JPEG image codec is shown in Fig. 3. The basic processes are similar to the DCT-JPEG algorithm. The differences between them are the transform (DCT or WAPBT) and quantizer (quantization table or uniform quantization step). Other steps of image compression algorithm are identical to DCT-based JPEG. Besides, the scheme of WAPBT-JPEG image codec is totally identical to APBT-based JPEG except the transform process (APBT or WAPBT).

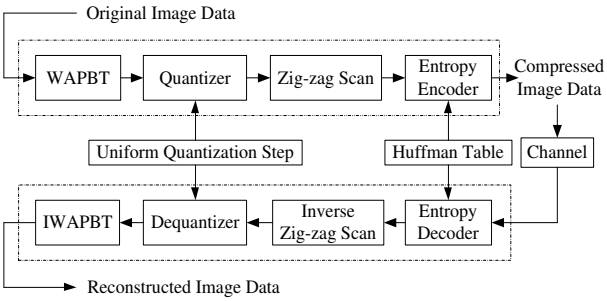

Fig. 3. The proposed scheme of WAPBT-JPEG image codec.

B. Generalized Pattern Search Algorithm (GPSA)

Unconstrained optimization problem can be formulated as a D-dimensional minimization problem as follows:

$$Min\ f(\boldsymbol{x}),\ \boldsymbol{x}=[x_1,x_2,\cdots,x_D]^{\mathrm{T}} \tag{14}$$

where D is the number of the parameters to be optimized; f is the objective function and parameters vector $\boldsymbol{x}$ is considered to be a point in the D-dimensional real space $\boldsymbol{R}^D$. There is a relatively conventional optimization technique called generalized pattern search algorithm (GPSA), which is a typical direct search method proposed by Torczon in 1997 [19]. GPSA is reviewed by Lewis in 2000 [20].

GPSA is an iterative method that generates a sequence of feasible iterates whose objective function value is nonincreasing. At any given iteration, the objective function is evaluated at a finite number of points on a mesh in order to try to find one that yields a decrease in the objective function value.

Each iteration is divided into two phases: an optional search and a local poll [22].The first phase (called the search step) provides flexibility to the method and determines in practice the global quality of the solution; a user can do a more extensive search in hopes of finding a better local solution. The second phase (called the poll step) follows stricter rules and guarantees theoretical convergence to a local minimizer of a quality specified by the user.

A flow chart of generalized pattern search algorithm is shown in Fig. 4.

The process of GPSA can be summarized as the following steps:

Step 1. Set a point of beginning $\boldsymbol{x}_0 = [x_1, x_2, \cdots, x_D]$, and then an exploratory movement determined by mesh size M at $\boldsymbol{x}$ will conduct around the point in D-dimensional real space during each iteration.

Step 2. In the k-th iteration of GPSA, a search is an algorithm that runs before a poll. The search attempts to locate a better point $\boldsymbol{x}_k$ than the current point $\boldsymbol{x}_{k-1}$. (Better means one with lower objective function value $f(\boldsymbol{x}_k) < f(\boldsymbol{x}_{k-1})$.) If the search finds a better point, the better point becomes the current point, and no polling is done at that iteration. If the search does not find a better point, pattern search performs a poll.

Step 3. If a point $\boldsymbol{x}_k$ with a better objective function value than $\boldsymbol{x}_{k-1}$ is found in either phase above, then the k-th iteration is declared successful. The better point $\boldsymbol{x}_k$ becomes the new current point, and the next iteration is initiated with a coarser mesh M_k around the new current point. Otherwise, the k-th iteration is declared unsuccessful. The next iteration is initiated at the same current point $\boldsymbol{x}_k = \boldsymbol{x}_{k-1}$, but with a finer mesh $M_k^{'}$ around the current point, and a set of points visited will be closer to the current point in next iteration.

Step 4. The iteration of GPSA will be terminated, when a convergence condition is satisfied (such as mesh size less than pre-set value).

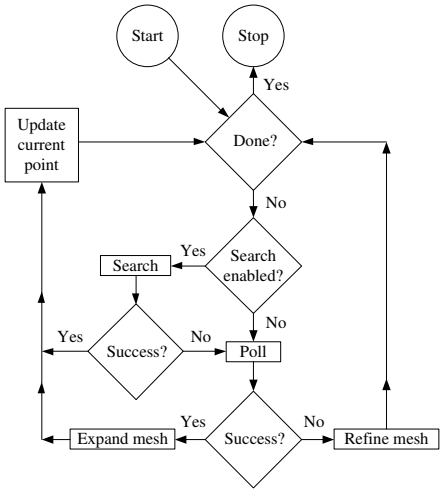

Fig. 4. The flow chart of generalized pattern search algorithm.

C. Obtain Optimal Window Sequence of WAPBT for Image Compression by GPSA

GPSA is an optimization technique that does not require gradient information of the objective function. And it is based on a simple concept that is easy to be implemented and is efficient when computed. Therefore optimal window sequence of WAPBT for image compression can be obtained by GPSA. Simulating in MATLAB, we can call MATLAB function called "pattern search" to implement GPSA for convenience.

The parameters to be optimized by GPSA are $\boldsymbol{B}^1(n)$ and $\boldsymbol{B}^2(n)$ ($N = 8$) that are organized into this form:

$$\boldsymbol{x} = [B_N^1(0), \cdots, B_N^1(N-1), B_N^2(1), \cdots, B_N^2(N-1)]^{\mathrm{T}} \quad (15)$$

Vector $\boldsymbol{x}$ is considered to be a point in the 16-dimensional real space $\boldsymbol{R}^{16}$. Firstly we set a point of beginning: $\boldsymbol{x}_0 = [1, 1, \cdots, 1]$. In WAPBT-JPEG image codec, PSNR is utilized as reconstructed figures of merit. Objective function f in GPSA is determined by PSNR of WAPBT-JPEG applied to image $\boldsymbol{I}$ at a bit rate BR.

$$f(\boldsymbol{x}) = -PSNR \quad (16)$$

That $\boldsymbol{\alpha} = \mathrm{IDCT}$ is adopted in WAPBT-JPEG in this paper, and comparing with $\boldsymbol{\alpha}$ being DCT or WHT, the performance of WAPBT-JPEG is best when $\boldsymbol{\alpha}$ is IDCT.

Flow chart of algorithm for obtaining optimal window sequence of WAPBT is shown in Fig. 5. In quantization phase of WAPBT-JPEG, "quality factor" Q is an important parameter in bit rate control. After each change of window sequence in GPSA, the corresponding quality factor Q will be found by golden-section search method [28] to fix the output bit rate at the pre-set value BR.

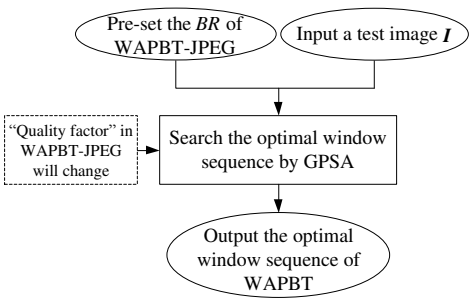

Fig. 5. The flow chart of algorithm for obtaining optimal window sequence of WAPBT.

In accordance with flow chart of algorithm shown in Fig. 5, a large number of experiments have been done with different input test image $\boldsymbol{I}$ and different output bit rate BR of WAPBT-JPEG. We hope to get simply optimal window sequence that does not increase the computational complexity. Thus, in the experiment, the minimum of mesh size in GPSA is set to value 1 so that integer window sequence will obtain in each experimental result. Experimental results show that, on a large number of natural images set, output results of the optimal window sequence at most of bit rates mainly focus on [8, 1, 2, 2, 1, 2, 1, -1, 1, 1, 1, 1, 1, 1, 1, 1]. However, output results of the optimal window sequence at lower bit rates mainly focus on [7, 6, 5, 5, 5, 5, 5, 4, 2, 7, 5, 5, 5, 5, 4, 5].

Finally, two kinds of optimal window sequence of WAPBT for image compression are obtained from experimental results. One of them is called WAPBT1 whose optimal window sequence is:

$$\begin{aligned} \boldsymbol{B}^1_{\mathrm{WAPBT1}} &= [7,\ 6,\ 5,\ 5,\ 5,\ 5,\ 5,\ 4]^{\mathrm{T}} \\ \boldsymbol{B}^2_{\mathrm{WAPBT1}} &= [2,\ 7,\ 5,\ 5,\ 5,\ 5,\ 4,\ 5]^{\mathrm{T}} \end{aligned} \quad (17)$$

The other is called WAPBT2 whose optimal window sequence is:

$$\boldsymbol{B}^1_{\text{WAPBT2}} = [2^3,\ 1,\ 2^1,\ 2^1,\ 1,\ 2^1,\ 1,\ -1]^{\text{T}}$$
$$\boldsymbol{B}^2_{\text{WAPBT2}} = [1,\ 1,\ 1,\ 1,\ 1,\ 1,\ 1,\ 1]^{\text{T}} \quad (18)$$

The DCT is a robust approximation of the optimal Karhunen-Loeve transform (KLT). With the assumption that the input signal is a first-order Gaussian-Markov process with zero-mean, unit variance, and correlation coefficient $\rho = 0.95$ (a good approximation for natural images), the coding gain of the DCT is very close to that of the optimal KLT [29]. Therefore, we hope that WAPBT has good decorrelation ability. There is a mathematical model called decorrelation efficiency η [30] used to measure decorrelation ability of transform.

$$\eta = 1 - \frac{\sum_{i,j=0,i\neq j}^{2N-1} |\boldsymbol{R}y|}{\sum_{i,j=0,i\neq j}^{2N-1} |\boldsymbol{R}x|},\ N = 8 \quad (19)$$

where $\boldsymbol{R}y$ and $\boldsymbol{R}x$ is correlation coefficients matrix calculated from transform coefficients blocks and image data blocks respectively. Each element in image data block and transform coefficients blocks is considered to be a random variable. In order to estimate $\boldsymbol{R}y$ and $\boldsymbol{R}x$, a set of 45 512×512 8bpp monochrome images obtained from a standard public image bank [31] is considered. Decorrelation ability comparison of DST, DCT, APBT and WAPBT applied to images is shown in Table I.

TABLE I: DECORRELATION ABILITY COMPARISON OF DST, DCT, APBT, AND WAPBT APPLIED TO IMAGES (A SET OF 45 GREYSCALE IMAGES).

Transform	Decorrelation Efficiency (%)
DST	0.9431
DCT	0.9881
APBT	0.9881
WAPBT1	**0.9890**
WAPBT2	0.9879

From Table I, what we can conclude is that the decorrelation ability of DCT, APBT and WAPBT is at a comparable high level.

JPEG-like image codec is a complex system that is composed of several parts including quantization and entropy encoder. Application of WAPBT in JPEG-like image compression is shown in the following section.

VI. EXPERIMENTAL RESULTS AND COMPARISONS WITH DCT-JPEG, APBT-JPEG AND WAPBT-JPEG

A. PSNR Comparison of DCT-JPEG, APBT-JPEG and WAPBT-JPEG

In order to test the proposed scheme and compare with the DCT-JPEG and APBT-JPEG algorithm, in this section, we will present simulation results obtained by applying the proposed transforms with optimal window sequence in Section V to test typical images Lena, Barbara, Flower, Peppers and Zoneplate, with the size of 512×512, 8bpp, monochrome images. Throughout this paper, all experiments are conducted with MATLAB7.0.

In the quantization part of APBT-JPEG algorithm and WAPBT-JPEG algorithm, the uniform quantization step (see Fig. 6(a)) is adopted. While in simple baseline DCT-JPEG algorithm, $\boldsymbol{C}$ is used in transform step with the quantization table (see Fig. 6(b)) suggested by JPEG. All of three methods use the typical Huffman tables (see [2]) which have been developed from the average statistics of a large set of images with 8-bit precision. The distortion is measured by the *PSNR*:

$$PSNR = 10\log_{10}\left(\frac{255^2}{MSE}\right)(\text{dB}) \quad (20)$$

where *MSE* denotes the mean squared error between the original and reconstructed images.

1	1	1	1	1	1	1	1
1	1	1	1	1	1	1	1
1	1	1	1	1	1	1	1
1	1	1	1	1	1	1	1
1	1	1	1	1	1	1	1
1	1	1	1	1	1	1	1
1	1	1	1	1	1	1	1
1	1	1	1	1	1	1	1

(a)

16	11	10	16	24	40	51	61
12	12	14	19	26	58	60	55
14	13	16	24	40	57	69	56
14	17	22	29	51	87	80	62
18	22	37	56	68	109	103	77
24	35	55	64	81	104	113	92
49	64	78	87	103	121	120	101
72	92	95	98	112	100	103	99

(b)

Fig. 6. The quantization table: (a) uniform quantization table used in APBT-JPEG and WAPBT-JPEG, and (b) quantization table suggested by JPEG used in DCT-JPEG.

Tables II and III show the experimental results with DCT-JPEG, APBT-JPEG, WAPBT1-JPEG and WAPBT2-JPEG in terms of PSNR at different bit rates, applied to image Lena and Barbara, respectively. From Tables II and III, we conclude that compared with DCT-JPEG algorithm at the same bit rates in terms of PSNR, the performance of WAPBT-JPEG algorithm is superior to conventional DCT-JPEG in image compression. In particular, among the four transforms, WAPBT2-JPEG has the best performance in most of bit rates; WAPBT1-JPEG always outgoing DCT-JPEG and APBT-JPEG at almost various bit rates, especially at low bit rates.

TABLE II: PSNR COMPARISON OF DCT-JPEG, APBT-JPEG, AND WAPBT-JPEG APPLIED TO IMAGE LENA.

Bit rate (bpp)	PSNR (dB)			
	DCT-JPEG	APBT-JPEG	WAPBT1-JPEG	WAPBT2-JPEG
0.15	26.62	27.23	**27.34**	27.15
0.20	29.23	29.44	**29.53**	29.43
0.25	30.83	30.95	**31.06**	31.04
0.30	32.00	32.05	32.14	**32.19**
0.40	33.66	33.71	33.83	**33.94**
0.50	34.77	34.87	34.98	**35.20**
0.60	35.62	35.79	35.89	**36.17**
0.75	36.63	36.88	36.98	**37.32**
1.00	37.93	38.22	38.34	**38.73**
1.25	39.00	39.27	39.39	**39.82**
1.50	39.93	40.17	40.32	**40.82**

TABLE III: PSNR COMPARISON OF DCT-JPEG, APBT-JPEG, AND WAPBT-JPEG APPLIED TO IMAGE BARBARA.

Bit rate (bpp)	PSNR (dB)			
	DCT-JPEG	APBT-JPEG	WAPBT1-JPEG	WAPBT2-JPEG
0.15	22.41	**22.80**	22.78	22.39
0.20	23.59	23.86	**23.88**	23.70
0.25	24.44	24.69	24.76	**24.88**
0.30	25.19	25.51	25.59	**25.86**
0.40	26.61	27.07	27.15	**27.59**
0.50	27.95	28.42	28.55	**29.18**
0.60	29.23	29.68	29.85	**30.62**
0.75	30.90	31.39	31.58	**32.42**
1.00	33.23	33.59	33.84	**34.85**
1.25	35.10	35.38	35.66	**36.78**
1.50	36.71	36.83	37.16	**38.38**

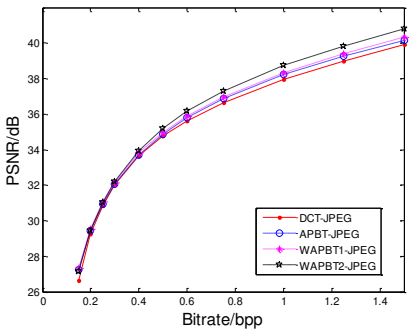

Fig. 7. The rate distortion curves of Lena.

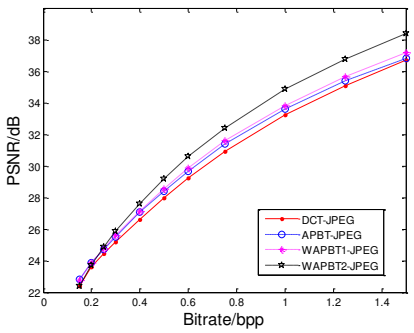

Fig. 8. The rate distortion curves of Barbara.

More simulation results are shown in Figs. 7~10. For the sake of clarity, we plot the rate distortion curves of Lena, Barbara, Flower and Peppers respectively.

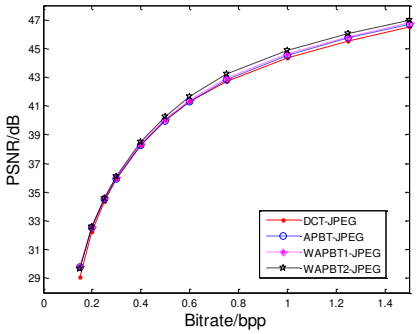

Fig. 9. The rate distortion curves of Flower.

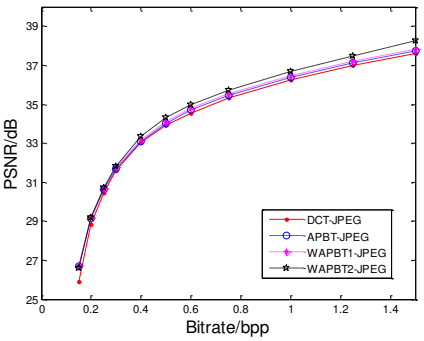

Fig. 10. The rate distortion curves of Peppers.

(a) (b) (c) (d)

Fig. 11. Lena obtained at 0.20bpp: (a) DCT-JPEG version, with PSNR=29.23dB, (b) APBT-JPEG version, with PSNR=29.44dB, (c) WAPBT1-JPEG version, with PSNR=29.53dB, and (d) WAPBT2-JPEG version, with PSNR=29.43dB.

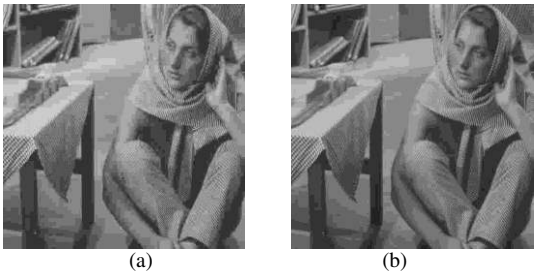

(a) (b)

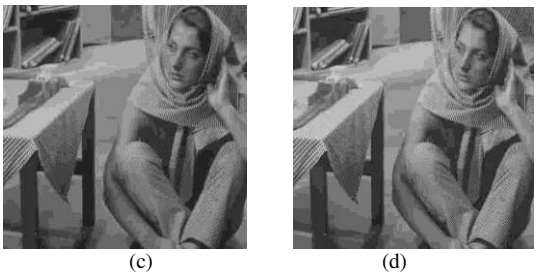

(c) (d)

Fig. 12. Barbara obtained at 0.30bpp: (a) DCT-JPEG version, with PSNR=25.19dB, (b) APBT-JPEG version, with PSNR=25.51dB, (c) WAPBT1-JPEG version, with PSNR=25.59dB, and (d) WAPBT2-JPEG version, with PSNR=25.86dB.

B. *Visual Quality of the Reconstructed Images of DCT-JPEG, APBT-JPEG and WAPBT-JPEG*

In order to compare the compression performance subjectively, Fig. 11~ Fig. 14 show the reconstructed image Lena, Barbara, Flower and Peppers of size 512×512 obtained by using DCT-JPEG, APBT-JPEG, WAPBT1-JPEG and WAPBT2-JPEG at some bit rates.

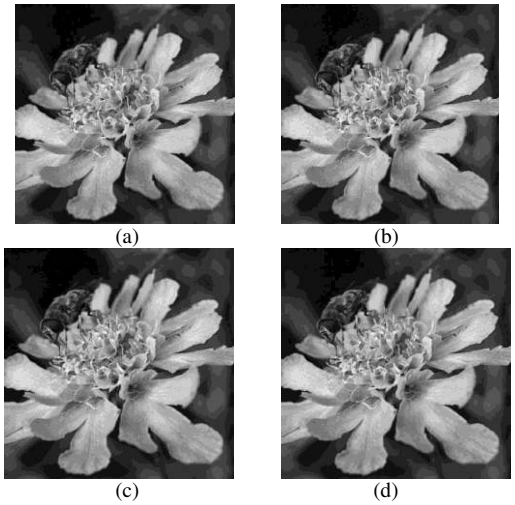

(a) (b)

(c) (d)

Fig. 13. Flower obtained at 0.75bpp: (a) DCT-JPEG version, with PSNR=42.71dB, (b) APBT-JPEG version, with PSNR=42.83dB, (c) WAPBT1-JPEG version, with PSNR=42.94dB, and (d) WAPBT2-JPEG version, with PSNR=43.21dB.

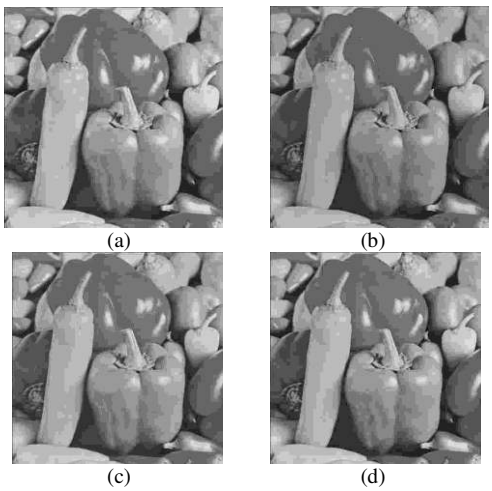

(a) (b)

(c) (d)

Fig. 14. Peppers obtained at 0.20bpp: (a) DCT-JPEG version, with PSNR=28.82dB, (b) APBT-JPEG version, with PSNR=29.15dB, (c) WAPBT1-JPEG version, with PSNR=29.21dB, and (d) WAPBT2-JPEG version, with PSNR=29.18dB.

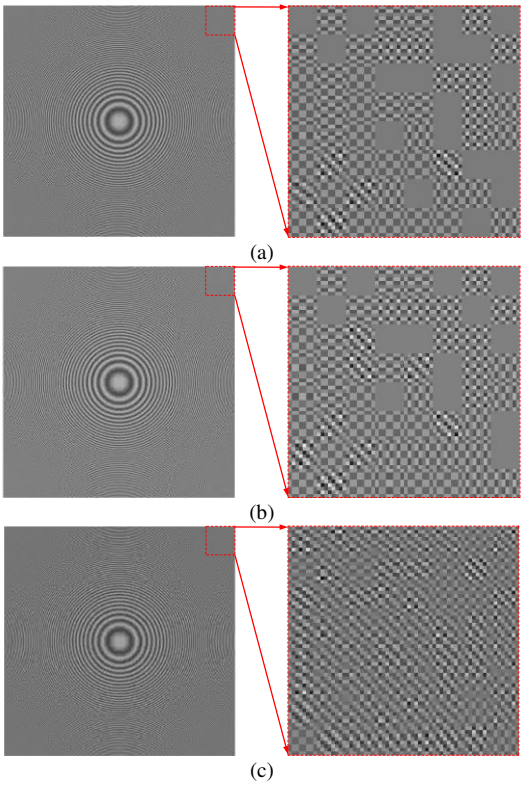

(a)

(b)

(c)

Fig. 15. Zoneplate obtained at 0.60bpp: (a) APBT-JPEG version, with PSNR=14.14dB, (b) WAPBT1-JPEG version, with PSNR=14.20dB, and (c) WAPBT2-JPEG version, with PSNR=14.79dB.

It is clear that, as compared with the DCT-JPEG version, better visual quality of APBT-JPEG and WAPBT-JPEG version is achieved and at lower bit rates, the blocking artifacts have been reduced. Besides, the difference of visual quality between the APBT-JPEG and WAPBT-JPEG version has shown in Fig. 15 in details (the reconstructed image Zoneplate of size 512×512 obtained by using APBT-JPEG, WAPBT1-JPEG and WAPBT2-JPEG at 0.60bpp). From the experimental results, we can see that compared with conventional DCT-JPEG, the proposed algorithm improves the performance at various bit rates, both in terms of PSNR and visual quality.

In the experiment, with all simulation results obtained by applying the WAPBT to 8bpp and monochrome images, there is a certain relationship between "Compression Ratio (CR)" and "Bit Rate (BR)" -- that is CR=8/BR. Therefore, we think it would be enough that all simulation results are summarized only on the basis of different bit rates. Finally, we would like to point out that the proposed scheme is also applied to other test images, and similar results can be obtained. Since the WAPBT-JPEG algorithm does not modify the basic compression algorithm, they can be used in other DCT-based codec without introducing substantial modifications.

VII. Conclusions

In this paper, the windowed all phase biorthogonal transform (WAPBT) and the matrices of WAPBT were deduced based on the theory of windowed all phase

digital filter. With optimal window sequence of WAPBT for image compression obtained by using GPSA, we successfully achieved the compression and reconstruction of image with WAPBT by replacing DCT which was commonly used in image compression. Compared with DCT-JPEG and APBT-JPEG, better performance was obtained. By inheriting good properties from APBT-JPEG, the advantage of the proposed algorithm was the simple quantization, taking uniform quantization for transform coefficients, especially saving much multiplication operations when adjusting the bit rates. A simpler and more effective algorithm is therefore developed, and can be easily implemented in both software and hardware.

In addition, we have not applied the proposed algorithm to other DCT-based schemes, such as MPEG-4, H.264/AVC, etc. Besides, we only discussed the application of the WAPBT in image compression. By finding proper window sequence of WAPBT, we can continue to explore other applications of WAPBT, such as image watermark, image retrieval, etc. These issues are left for future research. We can foresee that the proposed transforms will be widely used in the fields of image processing.

ACKNOWLEDGMENT

This work was supported by the National Natural Science Foundation of China (Grant No. 61201371) and the promotive research fund for excellent young and middle-aged scientists of Shandong Province, China (Grant No. BS2013DX022). The authors would like to thank Fanfan Yang and Xiaoyan Wang for their kind help and valuable suggestions. The authors would like to thank the anonymous reviewers and the editor for their valuable comments to improve the presentation of the paper.

REFERENCES

[1] N. Ahmed, T. Natarajan, and K. R. Rao, "Discrete cosine transform," *IEEE Trans. on Computers*, vol. 23, no. 1, pp. 90-93, Jan. 1974.

[2] ISO/IEC and ITU-T, "Information Technology—Digital Compression and Coding of Continuous-tone Still Images—Part 1: Requirements and Guidelines," ISO/IEC 10918-1 | ITU-T Rec. T. 81, 1st ed., Feb. 17, 1994.

[3] ISO/IEC, "Information Technology—Generic Coding of Moving Pictures and Associated Audio Information," ISO/IEC 13818, Apr. 25, 1995.

[4] T. Ebrahimi and C. Horne, "MPEG-4 natural video coding - an overview," *Signal Processing: Image Communication*, vol. 15, no. 4, pp. 365-385, Jan. 2000.

[5] Y. H. Seo, H. J. Choi, and D. W. Kim, "3D scanning-based compression technique for digital hologram video," *Signal Processing: Image Communication*, vol. 22, no. 2, pp. 144-156, Feb. 2007.

[6] A. Skodras, C. Christopoulos, and T. Ebrahimi, "The JPEG 2000 still image compression standard," *IEEE Signal Processing Magazine*, vol. 18, no. 5, pp. 36-58, Sep. 2001.

[7] S. K. Singh and S. Kumar, "Mathematical transforms and image compression: A review," *Maejo International Journal of Science and Technology*, vol. 4, no. 2, pp. 235-249, Jul. 2010.

[8] V. K. Bairagi, A. M. Sapkal, and M. S. Gaikwad, "The role of transforms in image compression," *Journal of The Institution of Engineers (India): Series B*, vol. 94, no. 2, pp. 135-140, Jun. 2013.

[9] Z. H. He, "Peak transform for efficient image representation and coding," *IEEE Trans. on Image Processing*, vol. 16, no. 7, pp. 1741-1754, Jul. 2007.

[10] M. H. Asghari and B. Jalali, "Discrete anamorphic transform for image compression," *IEEE Signal Processing Letters*, vol. 21, no. 7, pp. 829-833, Jul. 2014.

[11] E. Guzmaán, O. Pogrebnyak, C. Yanez, and L. P. S. Fernandez, "Morphological transform for image compression," *EURASIP Journal on Advances in Signal Processing*, pp. 15, Apr. 2008.

[12] F. M. Bayer and R. J. Cintra, "DCT-like transform for image compression requires 14 additions only," *Electronics Letters*, vol. 48, no. 15, pp. 919-921, Jul. 2012.

[13] U. S. Potluri, A. Madanayake, R. J. Cintra, F. M. Bayer, S. Kulasekera, and A. Edirisuriya, "Improved 8-point approximate DCT for image and video compression requiring only 14 additions," *IEEE Trans. on Circuits and Systems I: Regular Papers*, vol. 61, no. 6, pp. 1727-1740, Jun. 2014.

[14] R. J. Cintra and F. M. Bayer, "A DCT approximation for image compression," *IEEE Signal Processing Letters*, vol. 18, no. 10, pp. 579-582, Oct. 2011.

[15] Z. X. Hou, C. Y. Wang, and A. P. Yang, "All phase biorthogonal transform and its application in JPEG-like image compression," *Signal Processing: Image Communication*, vol. 24, no. 10, pp. 791-802, Nov. 2009.

[16] L. L. Zhao, "All phase digital filtering and image interpolation based on IDCT/DCT," Ph.D. thesis, Tianjin University, China, Jun. 2006. (in Chinese)

[17] Z. X. Hou, Z. H. Wang, and X. Yang, "Design and implementation of all phase DFT digital filter," *Acta Electronica Sinica*, vol. 31, no. 4, pp. 539-543, Apr. 2003.

[18] Z. X. Hou and N. N. Xu, "Windowed all phase DFT digital filter," *Journal of Tianjin University (Science and Technology)*, vol. 38, no. 5, pp. 448-454, May 2005.

[19] V. Torczon, "On the convergence of pattern search algorithms," *SIAM Journal on Optimization*, vol. 7, no. 1, pp. 1-25, Feb. 1997.

[20] R. M. Lewis, V. Torczon, and M. W. Trosset, "Direct search methods: Then and now," *Journal of Computational and Applied Mathematics*, vol. 124, no. 1-2, pp. 191-207, Dec. 2000.

[21] W. M. Li, Z. H. Jiang, T. L. Wang, and H. P. Zhu, "Optimization method based on generalized pattern search algorithm to identify bridge parameters indirectly by a passing vehicle," *Journal of Sound and Vibration*, vol. 333, no. 2, pp. 364-380, Jan. 2014.

[22] C. Audet and J. E. Dennis, "Pattern search algorithms for mixed variable programming," *SIAM Journal on Optimization*, vol. 11, no. 3, pp. 573-594, Feb. 2001.

[23] X. Zhou, X. Y. Wang, B. C. Jiang, and C. Y. Wang, "Adaptive threshold edge detection algorithm based on APDCSF and anti-symmetrical biorthogonal wavelet transform," *Journal of Communications*, vol. 9, no. 6, pp. 515-520, Jun. 2014.

[24] B. C. Jiang, A. P. Yang, C. Y. Wang, and Z. X. Hou, "Implementation of biorthogonal wavelet transform using discrete cosine sequency filter," *International Journal of Signal Processing, Image Processing and Pattern Recognition*, vol. 6, no. 4, pp. 179-189, Aug. 2013.

[25] Z. H. Wang and X. D. Huang, *All Phase Spectrum Analysis and Filtering Techniques for Digital Signal*, Beijing, China: Publishing House of Electronics Industry, Feb. 2009.

[26] L. L. Zhao and Z. X. Hou, "Windowed all phase digital filter based on IDCT," *Journal of Tianjin University (Science and Technology)*, vol. 39, no. 12, pp. 1499-1503, Dec. 2006.

[27] B. C. Jiang, A. P. Yang, C. Y. Wang, and Z. X. Hou, "Shape adaptive all phase biorthogonal transform and its application in

image coding," *Journal of Communications*, vol. 8, no. 5, pp. 330-336, May 2013.
[28] C. Gong and Z. L. Wang, *Proficient in Optimization Calculation with MATLAB*, 3rd ed., Beijing, China: Publishing House of Electronics Industry, Sep. 2014.
[29] R. J. Clarke, "Relation between the Karhunen Loeve and cosine transforms," *IEE Proceedings, Part F: Communications, Radar and Signal Processing*, vol. 128, no. 6, pp. 359-360, Nov. 1981.
[30] W. K. Cham, "Development of integer cosine transforms by the principle of dyadic symmetry," *IEE Proceedings, Part I: Communications, Speech and Vision*, vol. 136, no. 4, pp. 276-282, Aug. 1989.
[31] Signal and Image Processing Institute. (Mar. 22, 2015). The USC-SIPI Image Database. University of Southern California. USA. [Online]. Available: http://sipi.usc.edu/database/

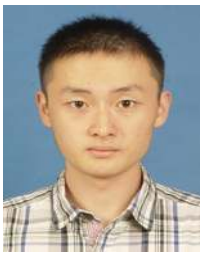

Qiming Fu was born in Jiangxi province, China in 1992. He received his B.S. degree in electronic information science and technology from Shandong University, Weihai, China in 2013. He is currently pursuing his M.E. degree in electronics and communication engineering in Shandong University, Weihai, China. His current research interests include digital image processing and transmission technology.

Xiao Zhou was born in Shandong province, China in 1982. She received her B.E. degree in automation from Nanjing University of Posts and Telecommunications, China in 2003, her M.E. degree in information and communication engineering from Inha University, Korea in 2005, and her Ph.D. degree in information and communication engineering from Tsinghua University, China in 2013. Now she is a lecturer in the School of Mechanical, Electrical and Information Engineering, Shandong University, Weihai, China. Her current research interests include wireless communication technology, digital image processing and analysis.

Chengyou Wang was born in Shandong province, China in 1979. He received his B.E. degree in electronic information science and technology from Yantai University, China in 2004, and his M.E. and Ph.D. degree in signal and information processing from Tianjin University, China in 2007 and 2010 respectively. Now he is an associate professor and supervisor of postgraduate in the School of Mechanical, Electrical and Information Engineering, Shandong University, Weihai, China. His current research interests include digital image/video processing and analysis, multidimensional signal and information processing.

Baochen Jiang was born in Shandong province, China in 1962. He received his B.S. degree in radio electronics from Shandong University, China in 1983 and his M.E. degree in communication and electronic systems from Tsinghua University, China in 1990. Now he is a professor in the School of Mechanical, Electrical and Information Engineering, Shandong University, Weihai, China. His current research interests include signal and information processing, image/video processing and analysis, and smart grid technology.